Numerical Study of Optical Frequency Combs in mid-IR Quantum Cascade Lasers: Effective Semiconductor Maxwell-Bloch Equations

Carlo Silvestri*, Lorenzo Columbo*, Massimo Brambilla**, Mariangela Gioannini*
* Dipartimento di Elettronica e Telecomunicazioni, Politecnico di Torino, Corso Duca degli Abruzzi 24, Torino, IT-10129, Italy
** Dipartimento Interateneo di Fisica, Politecnico ed Università degli Studi, Via Amendola 173, Bari, IT-70126, Italy
E-mail: carlo.silvestri@polito.it

***Abstract*—In this paper a theoretical model based on Effective Semiconductor Maxwell-Bloch Equations (ESMBEs) is proposed for the description of the dynamics of a multi-mode mid-Infrared (mid-IR) Quantum Cascade Laser (QCL) in Fabry Perot (FP) configuration, in order to investigate the spontaneous generation of frequency combs in this device. In agreement with recent experimental results our numerical simulations show both chaotic and regular multimode regimes. In the latter case we identify self-confined structures travelling along the cavity, and furthermore the instantaneous frequency is characterized by a linear chirp behaviour.**

I. Introduction

Optical frequency combs (OFC) consist in a set of equally spaced optical lines having constant phase difference and amplitudes. Since the first demonstration that QCLs can operate as sources of frequency combs [1], the study of the multi-mode dynamics of these lasers became relevant, for the development of applications in the field of e.g. molecular spectroscopy and optical communications [2]. Experimental studies have been conducted in both mid-IR and Terahertz (THz) spectral regions [1], [3], [4], [5]. Different classes of models have been proposed to interpret the experimental results, but only few of them [6], [7], correctly account for the effective refractive index profile in the frequency domain and non-zero linewidth enhancement factor (α-parameter) that play a fundamental role in QCL multi-mode dynamics.
In this work we discuss some relevant results on spontaneous OFC formation using a model which accurately extends the one introduced in [6] for a unidirectional ring cavity to the more standard FP configuration as described in [8] to account for Spatial Hole Burning (SHB).

II. The Model: Effective Semiconductor Maxell-Bloch Equations for a Fabry-Perot multimode QCL

We consider a FP cavity a few millimeters long and exploit a slowly varying envelope approximation for describing the spatio-temporal evolution of the electric field.
We retrieve then the ESMBEs:

$$\pm\frac{\partial E^{\pm}}{\partial z}+\frac{1}{v}\frac{\partial E^{\pm}}{\partial t} = -\frac{\alpha_L}{2}E^{\pm}+gP_0^{\pm} \quad (1)$$

$$\frac{\partial P_0^{\pm}}{\partial t}=\pi\delta_{hom}\left(1+i\alpha\right)\left[-P_0^{\pm}+F\left(N_0E^{\pm}+N_1^{\pm}E^{\mp}\right)\right] \quad (2)$$

$$\frac{\partial N_0}{\partial t} = \frac{I}{eV}-\frac{N_0}{\tau_e}-\frac{1}{2\hbar}Im\left[E^{+*}P_0^{+}+E^{-*}P_0^{-}\right] \quad (3)$$

$$\frac{\partial N_1^{+}}{\partial t} = -\frac{N_1^{+}}{\tau_e}+\frac{i}{4\hbar}\left[E^{-*}P_0^{+}-E^{+}P_0^{-*}\right] \quad (4)$$

where:

$$g = \frac{-i\omega_0 N_p\Gamma_c}{2\epsilon_0 nc}, \quad \delta_{hom}=\frac{1}{\pi\tau_{dt}},$$
$$F = if_0\epsilon_0\epsilon_b\left(1+i\alpha\right) \quad (5)$$

and where E^{+}, E^{-}, P_0^{+}, P_0^{-} are respectively the slowly varying envelope terms of forward and backward fields, and of forward and backward terms of polarization, N_0 is the zero-order carrier density term, which does not include the presence of the carrier grating, and N_1^{+} is the carrier density term related to the carrier grating caused by SHB [8]. The main parameters of the model are the total loss α_L, the Linewidth Enhancement Factor (LEF) α, the carrier nonradiative decay time τ_e, the semiconductor polarization dephasing time τ_{dt} and the homogeneous contribution to the Full Width at Half Maximum (FWHM) of the gain curve at threshold δ_{hom}. The other parameters are the active region volume V, the number of cascading stages N_P, the length of the cavity L, the differential gain f_0, the laser facet reflectivity R, the effective refractive index n, and the pump current I.

III. Simulation Results

In this section we present the most relevant simulation results obtained by numerical integration of the ESMBEs. Our first aim was the reproduction of OFC with analogies with the available experimental results. Fixing the model parameters, as from Table 1, we scanned the pump current from I_{thr} to $3I_{thr}$. We also consider $\alpha=0.4$ and $\delta_{hom}=0.48$THz.

Table 1. Typical parameters for a FP QCL

n	L(μm)	R	τ_d(ps)	τ_e(ps)	Γ_c	fo(μm^3)	V(μm^3)	N_P	λo(μm)
3.3	2000	0.3	0.1	1	0.3	1.1*10^{-7}	2240	50	10

978-1-7281-6086-3/20/$31.00 ©2020 IEEE

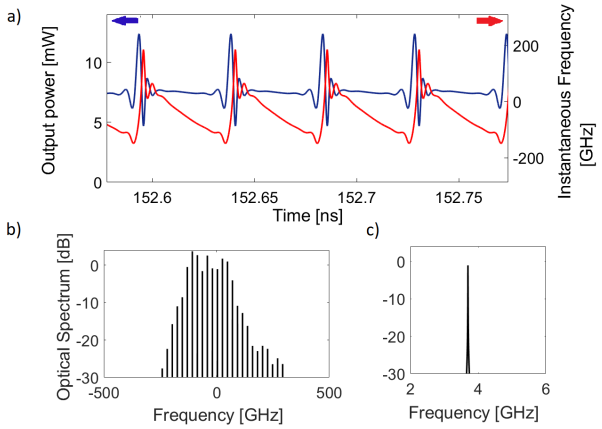

Fig. 1. Example of OFC emission at I=2.31I_{thr}. Temporal evolution of laser power (blue curve) and instantaneous frequency (red curve). (b) Optical spectrum with 10 modes in the $-10dB$ bandwidth. c) Zoom around one peak of the optical spectrum.

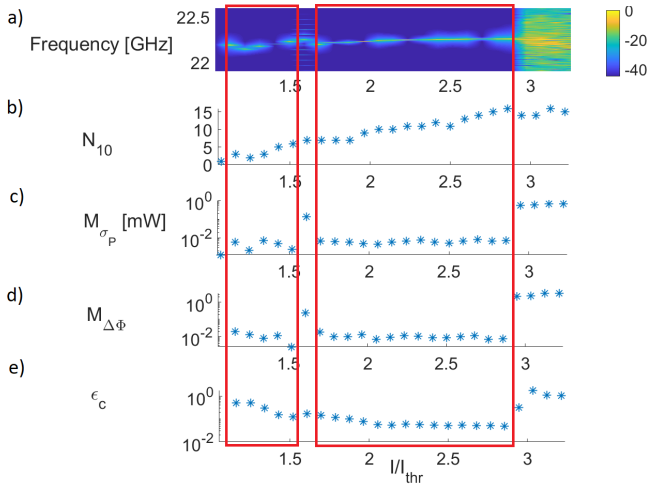

Fig. 2. Results for a current scan from I_{thr} to $3I_{thr}$ for $\alpha = 0.4$, $\delta_{hom} = 0.48THz$. a) First BN in the RF spectrum; b) number of modes in the -10dB bandwidth; (c) amplitude and (d) phase noise quantifiers. Two regions of OFCs operation are highlighted with a red box; (e) chirp quantifier.

The first result we present is a dynamical behaviour corresponding to the self-starting OFC, which is shown in Fig. 1. The power dynamics is characterized by confined structures propagating at the group velocity in the FP cavity and the instantaneous frequency of the laser shows a linear chirp corresponding to the constant intensity background and fast, discontinuous jumps when the intensity structure occur (Fig. 1.a). This shows a strong similarity with the experimental results presented in Fig. 2.b of [5]. In Fig.1.b and 1.c we show respectively the optical spectrum and a zoom around one peak of the optical spectrum.

For the characterization of OFCs regimes we introduce quantifiers for the modal power fluctuations (M_{σ_P}) and intermode phase jitter ($M_{\Delta\Phi}$), that have been recently introduced for the study of OFCs in QD lasers [8]. The OFC regime is characterized by low intensity and phase noise; we identify it as the case when $M_{\sigma_P} < 10^{-2}$ mW and $M_{\Delta\Phi} < 10^{-2}$ rad. To quantify the presence of a linear chirp, we introduce the chirp indicator ϵ_c, which evaluates the relative error between the instantaneous frequency signal and a perfect sawtooth signal (ideal case of linear frequency modulation). Similarly, we consider that $\epsilon_c < 10^{-1}$ will indicate a significant portion of linear chirping in the instantaneous frequency evolution.

In figure 2 we show the results when the current I is swept between I_{thr} and $3I_{thr}$. The amplitude and phase noise indicators, Fig.2.b and 2.c respectively, mark two locking windows, boxed in red. In the intermediate region, the system is chaotic and coherently the indicators show strong power and phase noise, with no linear chirping.

In order to highlight the role of the LEF and effective refractive index dispersion bandwidth in affecting both the bias current range of OFC regime and the properties of OFCs we run sistematic sets of simulations by sweeping the bias current between I_{th} and $3I_{th}$. Our results are summarized in Fig.3. As a general trend, in the locked regime the number of locked modes tends to increase with the FWHM of the gain curve

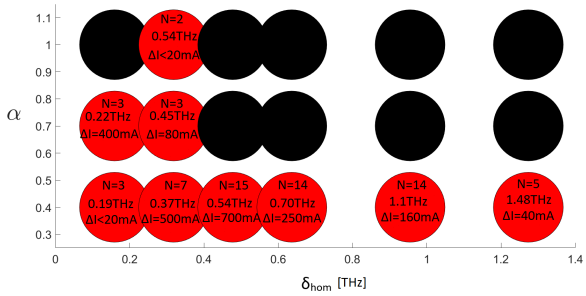

Fig. 3. Regimes upon variation of δ_{hom} and α. Black and red circles indicate unlocked and locked (OFC) regime respectively. OFC regime is quantified by the number of modes N, gain FWHM and bias current range reported in the circles.

and, for a fixed value of δ_{hom}, larger values of α reduce the range of ΔI in agreement with the results in [6].

IV. Conclusion

We discussed simulation results using a model for a QCL in FP configuration, which includes SHB and the characteristics of a semiconductor active medium. Thanks to this model we can well reproduce experimental findings on OFC formation and we can predict the role of α and gain spectral bandwith in this phenomenon.

References

[1] A. Hugi et al., Nature **492**, 229–233 (2012).
[2] J. Faist et al., Nanophotonics **5**, 272–291 (2016).
[3] M. Rösch et al., Nat. Photon. **9**, 42–47 (2015).
[4] H. Li et al., Opt. Express **23**, 33270–33294 (2015).
[5] M. Singleton et al., Optica **5**, 948-953 (2018).
[6] L. L. Columbo et al., Opt. Express **26**, 2829-2847 (2018).
[7] N. Opacak et al., Phys. Rev. Lett. **23**, 243902 (2019).
[8] P. Bardella et al., Opt. Express **25**, 26234-26252 (2017).